CHEMICAL REACTOR DESIGN FOR PROCESS PLANTS

Volume Two: Case Studies and Design Data

HOWARD F. RASE

W. A. Cunningham Professor of Chemical Engineering
The University of Texas at Austin

Original Illustrations by

JAMES R. HOLMES

Associate Professor of Engineering Graphics
The University of Texas at Austin

A WILEY-INTERSCIENCE PUBLICATION

JOHN WILEY & SONS, New York • London • Sydney • Toronto

CASE STUDY 110

Phthalic Anhydride Production

THIS is a classic example of a rapid oxidation reaction which if not controlled, produces CO and CO_2 rather than the desired product. A multitubular reactor is essential and techniques for obtaining nearly complete conversion without causing a runaway must be developed.

The kinetic data used as representative of bench-scale studies have been presented previously for modeling studies as a means for discussing reactor models (4). The source and limitations of the data were not discussed. These data, however, are useful for this study since they have been employed previously in model studies and the present case study can add to the background already so expertly presented (4).

Problem Statement

An existing plant for producing phthalic anhydride from naphthalene is to be converted to *o*-xylene feed. The reactor consists of 2500 tubes, 2.5 cm ID and with a packed catalyst bed height of 3 m. The heat-transfer medium circulating outside the tubes is a sodium nitrite-potassium nitrate, fused-salt (HTS, heat-transfer salt). The elevated temperatures (350–400°C) required for these reactions make the use of boiling water impractical because of the high shell-side pressures that would be required. Steam is generated, however, in water cooling coils that are located in the fused-salt bath. The fused salt is continuously agitated by a mechanical stirrer (5). During the days of Houdry fixed-bed cracking of petroleum much experience was gained with heat-transfer salt, and it has been documented (6,7).

A pilot plant, consisting of a molten-salt bath containing one tube of the same dimensions as those in the large reactor, has been constructed and a new

catalyst has been studied briefly using *o*-xylene as the feed. At a mass velocity, $G = 4684$ kg/m^{2}hr necessary to maintain the desired production of phthalic anhydride in existing reactors at complete conversion of xylene and maximum selectivity, it was found impossible with the new catalyst to reach a conversion over 67% in the 3-m length at 360°C. Raising this temperature any significant amount caused reaction runaway.

Some preliminary bench-scale studies with the new catalyst have yielded some rate data that can be used for modeling this system.

Develop a model and test it at the pilot-plant conditions. Consider means for overcoming the production problem with the new catalyst and test these with the model. Ideas which are indicated to be valid by calculation and which, of course, make physical sense can then be confirmed on the pilot plant.

Chemistry

Overall Reactions

$$C_8H_{10} + 3O_2 \longrightarrow C_8H_4O_3 + 3H_2O;$$

$$C_8H_{10} + 10\tfrac{1}{2}O_2 \longrightarrow 8CO_2 + 5H_2O)$$

The oxidation of *o*-xylene occurs on V_2O_5 catalyst with good selectivity for phthalic anhydride, provided temperature is controlled within relatively narrow limits. To avoid explosive mixtures the *o*-xylene content of the feed stream of air and *o*-xylene should not exceed one percent.

The catalyst is thought to change oxidation states during the reaction such that the reduced form adds oxygen which in turn oxidizes the hydrocarbon, returning the catalyst to the reduced state (1). The total reaction scheme is quite complex and involves series and parallel reactions, as suggested in Fig. CS-10.1 (3). Side reactions to maleic anhydride and benzoic acid, which are not shown, produce the major byproducts other than CO and CO_2. The intermediates TA and PI are not present in the product at high conversions of *o*-xylene.

Catalyst Properties

Most catalysts for *o*-xylene and naphthalene oxidation contain V_2O_5 as the active component. Various improved catalysts have been introduced which give longer life and better selectivity. One type with good selectivity employs a low area inert support such as α-alumina with a bulk density of 1.3 g/cm^3. It consists of 0.3-cm spheres and has a 10% V_2O_5 content.

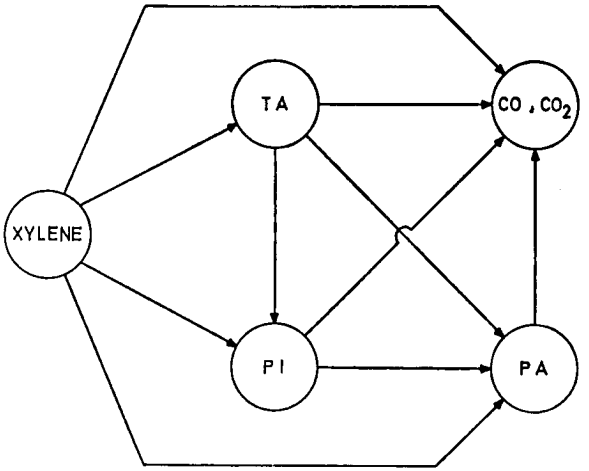

Fig. CS-10.1 Phthalic anhydride reaction scheme (TA = *o*-tolualdehyde, PI = phthalide, PA = phthalic anhydride). Reproduced by permission: J. Herten, and G. F. Froment, *Ind. Eng. Chem. Process Des. Develop.*, **7**, 517 (1968). [Copyright by the American Chemical Society.]

Thermodynamics

The reactions are highly exothermic. From Table 6.4 the high adiabatic factors (378 and 1344) and heat-generation potentials (12.8 and 48.3) confirm the need for heat-transfer reactors. Careful control is necessary to avoid ranges of temperature where total oxidation becomes dominate because of the extreme exothermicity of this reaction. A fluidized-bed reactor with internal heat-transfer surface is an alternate to the fixed-bed, multitubular reactor, and both have been successfully employed.

Safety

Feed composition must not exceed 1 mole % *o*-xylene in air so that an explosive mixture is avoided.

Kinetics

The oxidation of organic compounds such as *o*-xylene is highly complex. Models for the disappearance of *o*-xylene have been presented, one involving a steady-state oxidation–reduction assumption (1) and the other a steady state with equality of rate of oxygen adsorption and rate of reaction (2).

Both of these yield the same form of rate equation. As is often the case, the fit of experimental data does not resolve a mechanistic search.

For practical purposes more than just the rate of disappearance of *o*-xylene is needed. In order to model the highly temperature sensitive system at the very least the competition between PA production and complete oxidation must be followed. The complete oxidation causes extremely large heat effects which cannot be ignored.

It is necessary, as in all such complex systems, to simplify the structure of Fig. CS-10.1 to the following (4):

$$\text{o-xylene} \xrightarrow{(\text{air})k_1} \text{PA} \xrightarrow{(\text{air})k_2} \text{CO}_2 + \text{CO}$$

$$\text{o-xylene} \xrightarrow{(\text{air})k_3} \text{CO}_2 + \text{CO}$$

The corresponding rate expressions and rate constants are (4):

$$\hat{r}_1 = \hat{k}_1 P_A P_O; \ln k_1 = \frac{-27{,}000}{R'T} + 19.837 \qquad \text{(CS-10.1)}$$

$$\hat{r}_2 = \hat{k}_2 P_B P_O; \ln k_2 = \frac{-31{,}000}{R'T} + 20.86 \qquad \text{(CS-10.2)}$$

$$\hat{r}_3 = \hat{k}_3 P_A P_O; \ln k_3 = \frac{-28{,}600}{R'T} + 18.97 \qquad \text{(CS-10.3)}$$

where A is the *o*-xylene, B is phthalic anhydride, O is the oxygen, and rates are in terms of kg moles converted/(kg cat.)(hr).

Equations CS-10.1–CS-10.3 can be rewritten in terms of conversion (4).

Basis: 1 mole *o*-xylene and constant mole fraction of oxygen (O_2 is present in large excess)

$$\hat{r}_B = \hat{r}_1 - \hat{r}_2 = P^2 y_{O_0} y_{A_0} [k_1(1 - X_B - X_C) - k_2 X_B] \qquad \text{(CS-10.4)}$$

$$\hat{r}_C = \hat{r}_2 + \hat{r}_3 = P^2 y_{O_0} y_{A_0} [k_2 X_B + k_3(1 - X_B - X_C)] \qquad \text{(CS-10.5)}$$

where X_B is net moles PA (B) formed per mole *o*-xylene (A) charged, X_C is moles xylene converted to CO and CO_2 per mole *o*-xylene (A) charged.

Design Model for Heat-Transfer Reactor

For illustrative purposes both a one-dimensional and two-dimensional model will be used. The strategy illustrated here will be to make preliminary calculations with a one-dimensional model followed by estimates of the probable uncertainties due to interphase resistances and radial gradients.

Whatever these results show, a two-dimensional model will also be used to illustrate its application and to compare the results directly. In addition the algorithm developed here for the two-dimensional model will be compared with the published study which used the same data but a different algorithm.

One-Dimensional Model

Equations 9.3B and 9.4A of Table 9.1 for plug flow and negligible interphase gradients can be written in terms of the appearance of PA and CO + CO_2 with an inerts term added if the bed is diluted with inert support.

$$\frac{dX_B}{dZ} = \frac{M_F \hat{r}_B \rho_b}{y_{A_0} G(1 + \boldsymbol{b}_I)} \tag{CS-10.6}$$

$$\frac{dX_C}{dZ} = \frac{M_F \hat{r}_C \rho_b}{y_{A_0} G(1 + \boldsymbol{b}_I)} \tag{CS-10.7}$$

$$\frac{dT}{dZ} = -\frac{4U}{DGc_p}(T - T_j) + \frac{\rho_b\left(\frac{\hat{r}_B}{1 + \boldsymbol{b}_I}\right)(-\Delta H_B)}{Gc_p} + \frac{\rho_b\left(\frac{\hat{r}_C}{1 + \boldsymbol{b}_I}\right)(-\Delta H_C)}{Gc_p} \tag{CS-10.8}$$

where $\boldsymbol{b}_I$ is the mass of inerts per unit mass of catalyst.

The high heat-transfer coefficients obtainable with molten salts allows one to neglect the shell-side resistance along with the metal tube wall in comparison with the internal heat-transfer resistance.

Hence $h_T = h_w$.

From Eq. 11.53

$$\frac{1}{U} = \frac{1}{h_w} + \frac{D}{8\lambda_r} \tag{CS-10.9}$$

The values of h_w and λ_r given in Ref. 4 will be used so that the calculations can be compared. These values are slightly different from those that would be determined from the more recent correlation given in Appendix D. At $G = 4684$ kg/m^{2}hr, $h_w = 134$ kcal/m^{2}hr°C, and $\lambda_r = 0.67$ kcal/mhr°C from which $U = 82.7$ kcal/m^{2}hr°C. Other required data are $\Delta H_B = -307$ kcal/g mole xylene to PA, $\Delta H_C = -1{,}090$ kcal/g mole xylene to CO and CO_2, $y_{A_0} = 0.0093$, $y_{O_0} = 0.208$, $\rho_b = 1300$ kg/m^3, $D_p = 0.003$ m, $D = 0.025$ m, $c_p = 0.25$ kcal/kg °C and $M_F = 29.48$.

Equations CS-10.6–CS-10.8 were solved using a conventional difference scheme. Values of R_q (Eq. 11.58) were calculated at each increment. The average rate for the first increment was estimated from $(r_B)_1 = (r_B)_0 + 0.04$

ΔZ and $(r_C)_1 = (r_C)_0 + 0.07\,\Delta Z$. At other increments $\bar{r} = (r_{n-2} - r_{n-1})(\frac{1}{2}) + r_{n-1}$. The ΔT, ΔX, and ΔW for the increment were calculated and then the average rate recalculated and an iteration on temperature, conversion, and rate followed until convergence occurred.

Because of the long life of V_2O_5 catalyst, it is reasonable to consider diluting the bed with inerts or employing a less active form in the early portion of the bed in order to avoid excessive hot spots. Both of these techniques are included in existing patents on specific catalysts for this process (9,10). In employing either of these strategies the goal is to increase inlet and cooling temperatures so that complete conversion can be realized. The higher activation energy for the side reactions, however, definitely limits the extent of this increase.

Results with One-Dimensional Model

The results of several strategies are summarized in Table CS-10.1 and Fig. CS-10.2. With a value of $q_p = 48.3$ as maximum and values of R_q exceeding unity only near temperature maxima and then not greatly, the one-dimensional model should be reasonably valid. This is especially true for those cases removed from runaway (see p. 543[1]).

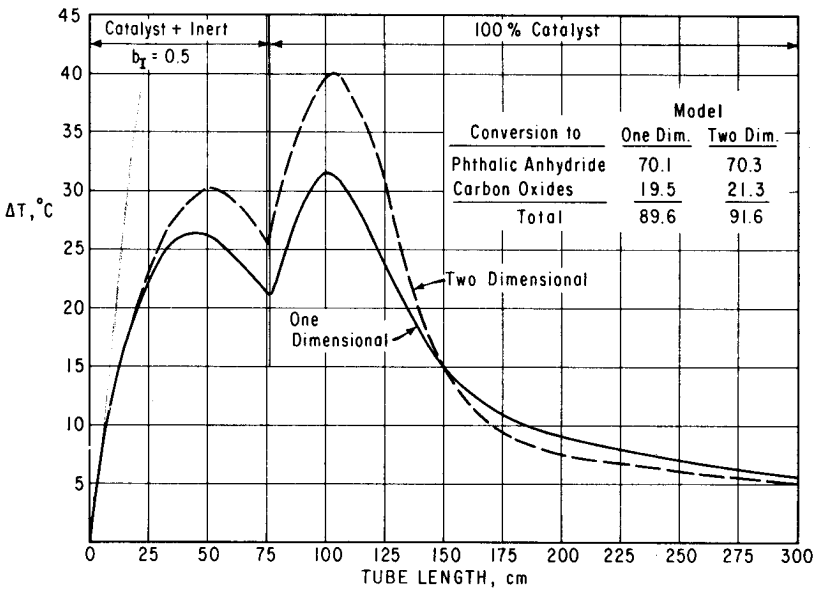

Fig. CS-10.2 Temperature profiles. (Alternate 6.)

Table CS-10.1 Alternate Designs for Phthalic-Anhydride Reactor[a]

Alternate Number	Inert Distribution	Inlet Temp. °C	Conversion[b] to Phthalic Anhydride	Conversion[b] to CO and CO_2	Total Conversion	% Selectivity[c]	Yield Lb PA per 100 Lb *o*-xylene
1	0	357	0.6377	0.1277	0.7654	83.32	89.04
2	0	360	0.6692	0.1486	0.8178	81.83	93.44
3	0	365	Runaway				
4	$b_I = 0.5$ in first $\frac{1}{2}$ $b_I = 0$ in last $\frac{1}{2}$	375	0.7017	0.2101	0.9118	76.96	97.97
5	$b_I = 0.5$ for 1st $\frac{1}{4}$ $b_I = 0$ in last $\frac{3}{4}$	375	0.7016	0.2382	0.9398	74.65	97.96
6	$b_I = 0.5$ for 1st $\frac{1}{4}$ $b_I = 0$ in last $\frac{3}{4}$	370	0.7010	0.1949	0.8959	78.25	97.86
7	$b_I = 0.5$ for first $\frac{1}{2}$ $b_I = 0$ for last $\frac{1}{2}$	380	Runaway				

[a] Reactor tube length is 3 m.

[b] Moles *o*-xylene converted to indicated product per mole of xylene charged.

[c] Selectivity = (conversion to PA)/(total conversion).

Alternate 6 in Table CS-10.1 is recommended as the best course of action involving charging $\frac{3}{4}$'s of the downflow reactor length with catalyst and the remaining top $\frac{1}{4}$ with a 50–50 mixture of catalyst and inert support. This causes two smaller hot spots instead of one larger uncontrollable temperature surge and a high enough temperature may thus be used to assure high conversion of *o*-xylene. The residual xylene may be consumed in a second reactor operated to ensure conversion rather than selectivity, or the residual gases may be used as an energy source.

Two-Dimensional Model

Since the one-dimensional model requires far less computing time, it is preferred for exploratory work. It is always feasible to check the crucial decisions thus reached using a two-dimensional model for comparison.

Equations 9.20 and 9.21 can be applied to this system with boundary conditions, as given on p. 408[1].

$$\frac{\partial X_B}{\partial Z} = \frac{\mathscr{D}_r \rho_f}{G}\left(\frac{\partial^2 X_B}{\partial \mathbf{r}^2} + \frac{1}{\mathbf{r}}\frac{\partial X_B}{\partial \mathbf{r}}\right) + \frac{\hat{r}_B \rho_B M_F}{G y_{A_0}} \qquad \text{(CS-10.10)}$$

$$\frac{\partial X_C}{\partial Z} = \frac{\mathscr{D}_r \rho_f}{G}\left(\frac{\partial^2 X_C}{\partial \mathbf{r}^2} + \frac{1}{\mathbf{r}}\frac{\partial X_C}{\partial \mathbf{r}}\right) + \frac{\hat{r}_C \rho_B M_F}{G y_{A_0}} \qquad \text{(CS-10.11)}$$

$$\frac{\partial T}{\partial Z} = \frac{\lambda_r}{G c_p}\left(\frac{\partial^2 T}{\partial \mathbf{r}^2} + \frac{1}{\mathbf{r}}\frac{\partial T}{\partial \mathbf{r}}\right) + \frac{\rho_B(-\Delta H_B)}{G c_p}\hat{r}_B + \frac{\rho_B(-\Delta H_C)}{G c_p}\hat{r}_C \qquad \text{(CS-10.12)}$$

The rate terms should be divided by $1 + b_1$ when inert solids are used.

The difference equations were derived by, as earlier suggested (11), transforming the radial coordinate of the differential equations which all have the same dimensionless form. The complex derivation yielded the following equations (12).

General Dimensionless Equation

$$\frac{\partial y}{\partial Z_a} = a_i\left[\frac{1}{\mathbf{r_a}}\frac{\partial y}{\partial \mathbf{r_a}} + \frac{\partial y}{\partial \mathbf{r_a}}\right] + S_i$$

where y refers to variable X_B, X_C, or $T_a = T - T_j$; $a_i = \mathscr{D}_r \rho_f / G D_p$ and $\lambda_r / G c_p D_p$ for heat balance equation; $\Delta Z_a = \Delta Z / D_p$, $\mathbf{r_a} = \mathbf{r}/D_p$, and $S_i = b_1 \hat{r}_B$ or $b_1 \hat{r}_C$ for mole balance and

$$\left[\frac{\rho_b D_p(-\Delta H_B)}{G c_p}\right]\hat{r}_B + \left[\frac{\rho_B D_p(-\Delta H_C)}{G c_p}\right]\hat{r}_C$$

for heat balance, and $b_1 = \rho_b D_p M_m / G y_{A_0}$. For interior of bed ($1 < n < N_E$, where N_E is the number of equal area radial increments):

$$y_{n,L+1} = y_{n,L} + \frac{2\Delta Z_a a_i}{\Delta u}[(2n-1)y_{n+1,L} + (2n-3)y_{n-1,L} - (4n-4)y_{n,L}] + \Delta Z_a S_i$$

where L and n are the number of axial and radial increments, respectively, and $u = \mathbf{r_a}^2$. For $n = 1$

$$y_{1,L+1} = y_{1,L} + \frac{2\Delta Z_a a_i}{\Delta u}(-3y_{1,L} + 4y_{2,L} - y_{3,L}) + \Delta Z_a S_i$$

For $n = N_E$:

$$y_{N_E,L+1} = y_{N_E,L} + \frac{8a_i \Delta Z_a}{\Delta u}\left[\frac{Dh_w T_a}{4\lambda_r}\delta_{T_a,y} - (N_E - \tfrac{3}{2})(y_{N_E,L} - y_{N_E-1,L})\right] + \Delta Z_a S_i$$

where $\delta_{T_a,y} = 0$ if $y \neq T_a$ and $= 1$ if $y = T_a$.

Results with Two-Dimensional Model

The algorithm for the two-dimensional model is similar to that described for the one-dimensional model. The difference equation routine was used to solve for T_a, X_B and X_C at each Z_a and r_a position. Stability was assured by maintaining $\Delta Z_a \leq \frac{1}{2}\Delta \mathbf{r_a}^2$. The equal area method with a six radial increments gives good agreement with the previously reported Crank-Nicholson method (4,8) while equal radial steps approach these solutions only at an impractical number of steps. The computing time using six equal-area increments was 5.68 sec for a 3-m tube.

The average radial temperature at various axial positions is plotted for alternate 6 in Fig. CS-10.2. Although these profiles do not exactly correspond, they are close enough to warrant using the one-dimensional model as the criteria given on p. 543[1] and applied on p. 128 already suggested. The slightly higher conversion to carbon oxides for the two-dimensional model is caused by the higher temperature excursion.

REFERENCES

1. P. Mars and D. W. van Krevelen, *Chem. Eng. Sci.*, **3**, 41 (1954).
2. J. A. Juusola, R. F. Mann, and J. Downie, *J. Catal.*, **17**, 106 (1970).
3. J. Herten and G. F. Froment, *Ind. Eng. Chem. Process. Des. & Develop.*, **7**, 516 (1968).

4. G. F. Froment, *Ind. Eng. Chem.*, **59**, 21 (1967).
5. E. Guccione, *Chem. Eng.* (*N.Y.*), p. 132 (June 7, 1965).
6. W. B. Johnson and W. M. Nagle, *Ind. Eng. Chem.*, **39**, 971 (1947).
7. R. H. Newton and H. G. Shimp, *Trans. A.I.Ch.E.*, **41**, 197 (1945).
8. G. C. Grosjean and G. F. Froment, *Ned. Kon. VI Acad. Belg.*, **24**, 1 (1962).
9. W. Friedrichsen and O. Goehre, (Badische Anilin u. Soda-Fabrik, A.G.) German Patent 2020482, Nov. 11, 1971.
10. W. R. Grace & Co. Brit. Patent 1280703, July 5, 1972.
11. J. Beek, *Adv. Chem. Eng.*, **3** (1962).
12. G. R. Dowling, private communication, 1972.